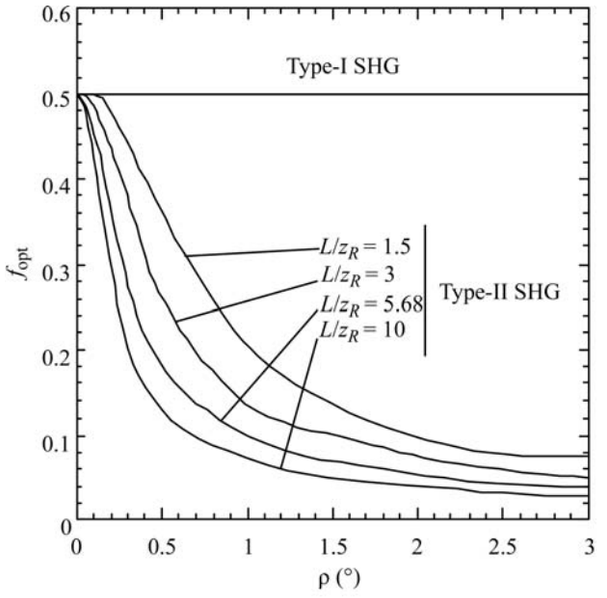

Fig. 1.7.3.12. Position f_{opt} of the beam waist for different values of walk-off angles and L/z_R, leading to an optimum SHG conversion efficiency. The value $f_{opt} = 0.5$ corresponds to the middle of the crystal and $f_{opt} = 0$ corresponds to the entrance surface (Fève & Zondy, 1996).

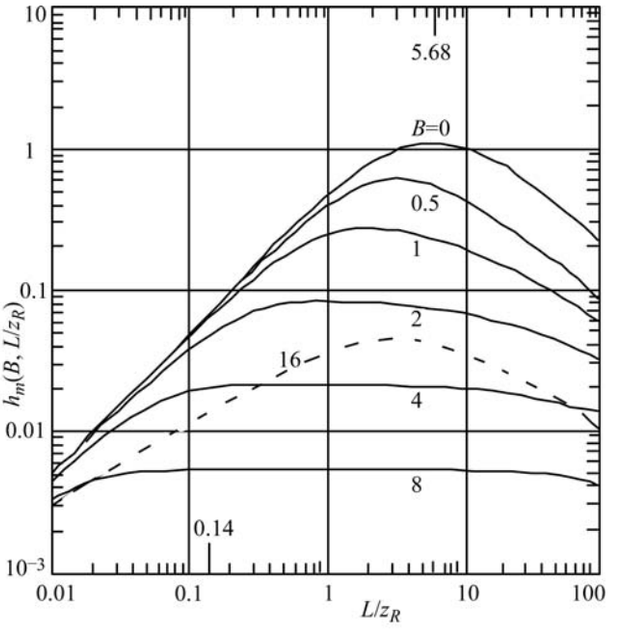

Fig. 1.7.3.13. Optimum walk-off function $h_m(B, L)$ as a function of L/z_R for various values of $B = (1/2)\rho\{[(k_o^\omega + k_e^\omega)/2]L\}^{1/2}$. The curve at $B = 0$ is the same for both type-I and type-II phase matching. The full lines at $B \neq 0$ are for type II and the dashed line at $B = 16$ is for type I. (From Zondy, 1990).

The computation of $h(L, w_o, \rho, f, \Delta k)$ allows an optimization of the SHG conversion efficiency which takes into account L/z_R, the waist location f inside the crystal and the phase mismatch Δk.

Fig. 1.7.3.12 shows the calculated waist location which allows an optimal SHG conversion efficiency for types I and II with optimum phase matching. From Fig. 1.7.3.12, it appears that the optimum waist location for type I, which leads to an optimum conversion efficiency, is exactly at the centre of the crystal, $f_{opt} = 0.5$. For type II, the focusing (L/z_R) is stronger and the walk-off angle is larger, and the optimum waist location is nearer the entrance of the crystal. These facts can be physically understood: for type I, there is no walk-off for the fundamental beam, so the whole crystal length is efficient and the symmetrical configuration is obviously the best one; for type II, the two fundamental rays can be completely separated in the waist area, which has the strongest intensity, when the waist location is far from the entrance face; for a waist location nearer the entrance, the waist area can be selected and the enlargement of the beams from this area allows a spatial overlap up to the exit face, which leads to a higher conversion efficiency.

The divergence of the pump beam imposes non-collinear interactions such that it could be necessary to shift the direction of propagation of the beam from the collinear phase-matching direction in order to optimize the conversion efficiency. This leads to the definition of an optimum phase-mismatch parameter Δk_{opt} $(\neq 0)$ for a given L/z_R and a fixed position of the beam waist f inside the crystal.

The function $h(L, w_o, \rho, f_{opt}, \Delta k_{opt})$, written $h_m(B, L)$, is plotted in Fig. 1.7.3.13 as a function of L/z_R for different values of the walk-off parameter, defined as $B = (1/2)\rho\{[(k_o^\omega + k_e^\omega)/2]L\}^{1/2}$, at the optimal waist location and phase mismatch.

Consider first the case of angular NCPM $(B = 0)$ where type-I and -II conversion efficiencies obviously have the same L/z_R evolutions. An optimum focusing at $L/z_R = 5.68$ exists which defines the optimum focusing $z_{R_{opt}}$ for a given crystal length or the optimal length L_{opt} for a given focusing. The conversion efficiency decreases for $L/z_R > 5.68$ because the increase of the 'average' beam radius over the crystal length due to the strong focusing becomes more significant than the increased peak power in the waist area.

In the case of angular CPM $(B \neq 0)$, the L/z_R variation of type-I conversion efficiency is different from that of type II. For type I, as B increases, the efficiency curves keep the same shape, with their maxima abscissa shifting from $L/z_R = 5.68$ $(B = 0)$ to 2.98 $(B = 16)$ as the corresponding amplitudes decrease. For type II, an optimum focusing becomes less and less appearent, while $(L/z_R)_{opt}$ shifts to much smaller values than for type I for the same variation of B; the decrease of the maximum amplitude is stronger in the case of type II. The calculation of the conversion efficiency as a function of the crystal length L at a fixed z_R shows a saturation for type II, in contrast to type I. The saturation occurs at $B \simeq 3$ with a corresponding focusing parameter $L/z_R \simeq 0.4$, which is the limit of validity of the parallel-beam approximation. These results show that weak focusing is suitable for type II, whereas type I allows higher focusing.

The curves of Fig. 1.7.3.14 give a clear illustration of the walk-off effect in several usual situations of crystal length, walk-off angle and Gaussian laser beam. The SHG conversion efficiency is calculated from formula (1.7.3.56) and from the function (1.7.3.57) at f_{opt} and Δk_{opt}.

1.7.3.3.2.3. *Non-resonant SHG with depleted pump in the parallel-beam limit*

The analytical integration of the three coupled equations (1.7.3.22) with depletion of the pump and phase mismatch has only been done in the parallel-beam limit and by neglecting the walk-off effect (Armstrong *et al.*, 1962; Eckardt & Reintjes, 1984; Eimerl, 1987; Milton, 1992). In this case, the three coordinate systems of equations (1.7.3.22) are identical, (X, Y, Z), and the general solution may be written in terms of the Jacobian elliptic function $\mathrm{sn}(m, \alpha)$.

For the simple case of type I, *i.e.* $E_1^\omega(X, Y, Z) = E_2^\omega(X, Y, Z) = E^\omega(X, Y, Z) = E_{tot}^\omega(X, Y, Z)/(2^{1/2})$, the exit second harmonic intensity generated over a length L is given by (Eckardt & Reintjes, 1984)

$$I^{2\omega}(X, Y, L) = I_{tot}^\omega(X, Y, 0) T^{2\omega} T^\omega v_b^2 \mathrm{sn}^2\left[\frac{\Gamma(X, Y)L}{v_b}, v_b^4\right]. \quad (1.7.3.58)$$